Experimental and Numerical Analysis of Reinforced Soil Retaining Walls with Poorly Graded Sand Backfill

D. Bahramiyan
University of Guilan, Rasht, Iran,bahramiyan.daniya@gmail.com

H. Ahmadi, P. Zanganeh Ranjbar
University of Guilan, Rasht, Iran, hadiahmadi@guilan.ac.ir, p.zanganeh@guilan.ac.ir

R. Jamshidi Chenari
TREK Engineering Inc.,Winnipeg, Canada (University of Guilan, Rasht, Iran), Jamshidi_reza@yahoo.com

B. Stuyts, M. Roustaei, M. Payan
Ghent University, Ghent, Belgium, bruno.stuyts@ugent.be, mahya.roustaei@ugent.be, meghdad.payan@ugent.be,

ABSTRACT: Reinforced soil retaining walls have gained widespread attention in geotechnical engineering as cost-effective and adaptable alternatives to conventional rigid retaining structures. Accurate prediction of their performance under realistic boundary and loading conditions remains challenging due to field-scale complexities, instrumentation limitations, and high experimental costs. This study presents a comprehensive investigation of the geotechnical behavior of reinforced soil walls constructed with poorly graded sand backfill using a well-instrumented laboratory-scale physical model. A transparent Plexiglas box (120×100×60 cm) was specially designed to enable real-time observation of soil deformation during loading. The effects of geogrid reinforcement layer arrangement were systematically examined, focusing on the perforation pattern. To complement the experimental program, a finite element model was developed in ABAQUS, replicating laboratory conditions and simulating wall behavior under similar loading scenarios. The results indicate that the reinforcement sheet with a P/3 perforation pattern significantly reduced horizontal displacement compared to the P/2 configuration, with a maximum displacement reduction of approximately 73% under identical surcharge conditions. Numerical and experimental results showed good agreement at upper and middle wall levels, whereas larger discrepancies were observed near the base, highlighting potential scale effects and boundary influences. The study demonstrates the critical role of reinforcement configuration in controlling deformations and enhancing structural performance. These findings provide valuable insights for the optimized design of reinforced soil walls, emphasizing the importance of perforation geometry, layer arrangement, and proper integration of reinforcement layers.

1 INTRODUCTION

Soils generally exhibit high compressive strength but low tensile resistance, which necessitates reinforcement to improve performance under tensile stresses (Albino et al., 2022; Bathurst & Simac, 1994). Reinforced soil systems offer numerous advantages, including reduced construction time and cost, ease of installation, minimal labor requirements, and adaptability to various wall dimensions. As a result, these systems have been widely applied in many infrastructure projects, such as bridge abutments, highway and railway retaining walls, slope stabilization, industrial platforms, and hydraulic structures. Incorporating reinforcement improves the tensile and shear strength of the soil, reduces lateral earth pressures, and enhances overall structural stability. These improvements are particularly crucial in applications where unreinforced soil exhibits excessive deformation, limited bearing capacity, or vulnerability to seismic forces.

Geogrids, a subset of geosynthetics, have emerged as widely used and highly effective reinforcement materials due to their durability, high resistance to chemical and biological degradation, and reliable performance under saturated conditions (Dewoolkar et al., 2015; Ehrlich et al., 2012). The effectiveness of geosynthetics, especially under dynamic and seismic loading, is more pronounced, making their integration into soil reinforcement a cost-effective, durable, and safe solution. Consequently, the use of geosynthetics in reinforced soil walls has expanded rapidly and is now considered a key approach in modern geotechnical engineering (Guler et al., 2007; Kim et al., 2020; Momeni et al., 2021; Yang et al., 2023; Vieira & Pereira, 2022; Bathurst and Jamshidi Chenari 2024). Several factors affect the performance of reinforced soil systems, including soil type, reinforcement properties, embedment length, overall safety factors, and compaction level (Liu et al., 2021; Soleimanbeigi et al., 2022; Pishgah and Jamshidi Chenar, 2024; Cai et al., 2025). Bathurst & Simac (1994) investigated the behavior of modular geosynthetic-reinforced walls in North America, reporting that geosynthetics improved wall stability, reduced deformations, and optimized stress distribution, thereby ensuring long-term performance and structural safety. Dash (2010) studied the effect of relative density on the performance of geocell-reinforced sand foundations, demonstrating that increased soil compaction significantly enhances bearing capacity and reduces settlement, with reinforcement effects being more pronounced in denser soils. Lee et al. (2010) evaluated the seismic behavior of geosynthetic-reinforced walls through numerical simulations and found that geosynthetic stiffness, wall height, and earthquake intensity significantly influence wall stability and deformation, emphasizing the importance of appropriate reinforcement type and layout for improved seismic response. Krishna & Latha (2012) numerically modeled the dynamic behavior of wrap-faced reinforced soil walls under seismic loading, using a nonlinear soil model and finite element method. Their results indicated that increasing the length and stiffness of reinforcement strips substantially improves wall stability and reduces permanent displacements. Portelinha et al. (2014) investigated the performance of woven and nonwoven geotextiles in reinforced sandy backfills under field conditions. Both types enhanced wall stability and reduced deformations, but woven geotextiles exhibited better performance in settlement control and stress distribution. Infante et al. (2016) studied geogrid-reinforced sand under vertical loading, showing that geogrid reinforcement increases sand strength and reduces vertical settlement, with reinforcement effects improving as the number of layers and embedment depth increase. Sharma & Kumar (2017) examined the influence of relative soil density on fiber-reinforced foundations, reporting that increased compaction enhances bearing capacity and reduces settlement, while fiber inclusion improves overall soil stability and shear strength. Yazdandoust (2017) evaluated the seismic performance of steel-strip reinforced soil walls using shake-table tests, showing that reinforced walls maintain high stability under earthquake loads, with displacement and stress distribution strongly influenced by strip stiffness and depth. Laboratory and numerical studies by Touahmia et al. (2018) demonstrated that geogrids increase soil bearing capacity and reduce surface settlement, with optimal effects achieved when geogrids are embedded at proper depths. Kayadelen et al. (2018) conducted laboratory pullout tests on geogrids in sand, reporting that geogrid properties and relative soil density significantly affect tensile resistance and pullout behavior, with higher density soils increasing pullout resistance and improving soil-reinforcement interaction. Zheng et al. (2019) studied semi-field scale geosynthetic-reinforced bridge foundations under dynamic loading, showing that reinforced systems provide adequate stability and damping, with displacements and deformations remaining within safe limits, highlighting the effectiveness of geosynthetics in enhancing seismic performance. Liu et al. (2021) calibrated simplified FHWA models for tensile forces in soil nail walls using field data and statistical analysis, indicating improved prediction accuracy and potential applications in wall design and safety assessment. Momeni et al. (2021) applied an optimized neural network with gravitational search algorithm to predict deformations of geogrid-reinforced earth structures, showing reliable and accurate predictions suitable for design and performance evaluation. Vieira & Pereira (2022) investigated the effect of geosynthetic type and compaction conditions on pullout behavior in recycled construction materials, demonstrating that proper selection of these parameters significantly improves reinforcement performance and system stability. Yang et al. (2023) analyzed the performance of geosynthetic-reinforced earth walls with marginal backfill under simulated rainfall using a model test, showing that geosynthetics effectively increase wall stability and reduce sliding and settlement caused by water infiltration, emphasizing the importance of appropriate geosynthetic type and layout in improving wet-condition performance.

In the present study, poorly graded silica sand was reinforced using four layers of continuous and perforated geogrid sheets with two different perforation arrangements. Medium-scale laboratory experiments were conducted with three LVDTs installed at the upper, middle, and lower elevations of the backfill to measure horizontal displacement. Subsequently, numerical modeling was performed based on the laboratory model using commercial software. Results demonstrated good agreement between numerical and experimental data at the middle and upper levels, while the P/3 perforation arrangement outperformed the alternative in terms of displacement reduction, highlighting the critical role of reinforcement layout in controlling deformation and improving structural performance of reinforced soil walls.

2 LABORATORY MODEL SPECIFICATIONS

A modular wall was modeled using 30 wooden facing units inside a glass box with internal dimensions of 120 × 100 × 60 cm (Figure 1). Each wooden facing block measured 2 × 3 × 59 cm and was stacked with an 8° backward inclination to simulate realistic field conditions. Wooden facing units were used to construct the modular wall system that reproduces the geometry of segmental retaining walls at a laboratory scale. The facing elements were carefully smoothed and finished to minimize surface roughness and reduce frictional interaction with the reinforcement layers, ensuring that the facing primarily served as a geometric boundary and did not artificially influence the deformation response of the wall. The stiffness of the wooden facing was significantly higher than the soil stiffness, preventing structural deformation of the facing itself. The experimental program was carried out under normal gravity (1g) laboratory. The purpose of adopting a 1g physical model was to investigate the deformation mechanism and comparatively evaluate the performance of different reinforcement perforation patterns under controlled boundary conditions. Wall displacements were measured using three Linear Variable Differential Transformers (LVDTs) installed at heights of 15 cm, 35 cm, and 55 cm from the base of the wall (Figure 2). Each LVDT had a resolution of 0.01 mm and a measurement range of up to 37 mm. All sensors were mounted on rigid steel brackets to ensure accuracy and stability of readings throughout the construction and loading phases.

To simplify the study of the reinforcing effect in the physical modeling of the embankment, Firouzkooh sand, which is classified as poorly graded sand (SP), was used. The physical properties of the sand are presented in Table 1, and the particle size distribution curve, determined according to ASTM D6913 (2007), is shown in Figure 3.

Figure 1. Glass box used for constructing the laboratory model.

Figure 2. Placement locations of the LVDTs

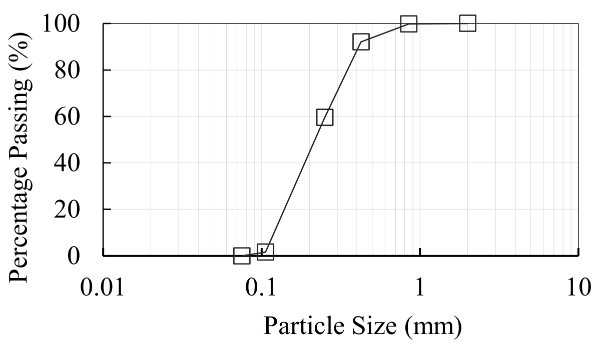

Figure 3. Grain size distribution of sand used in this study.

Table 1. Physical and mechanical properties of the tested sand.

Parameters	D_{10} (mm)	D_{30} (mm)	D_{50} (mm)	D_{60} (mm)	C_u	C_c	G_s	e_{max}	e_{min}	ω_{opt} (%)	φ (degree)	c (kPa)	k (m/s)
Values	0.42	0.58	0.77	0.90	2.14	0.89	2.65	0.9	0.6	11.2	39.2	5.5	0.0005

In the laboratory model, the reinforcing material consisted of Kraft paper with a basis weight of 70 g/m², and its mechanical properties are presented in Table 2. To investigate the effect of the geometry of the reinforcement and the arrangement of its perforations on the horizontal displacement of the wall, two reinforcement patterns were studied: the P/2 pattern, with a length-to-width ratio of the perforations equal to 2, and the P/3 pattern, with a length-to-width ratio of 3. The perforation pattern of the reinforcing sheets used is shown in Figure 4.

Table 2. Properties of the reinforcement materials.

Parameters	Elasticity modulus (MPa)	Tensile strength (N/cm^2)	Mass (g/cm^2)	Thicknes s (mm)
Values	195.8	33.6	0.0075	0.006

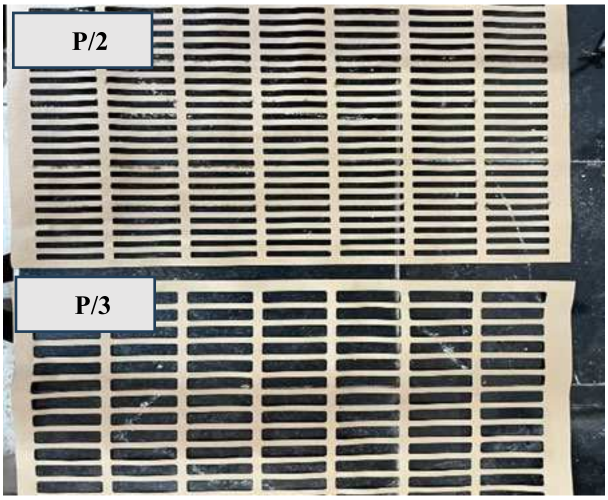

Figure 4. The perforation pattern of the reinforcing sheet.

The embankment was constructed using Firouzkooh sand at a relative density of 50%, to a height of 60 cm, with a facing slope angle of 8° and four reinforcement layers. The vertical spacing between the reinforcement layers was 150 mm, and the distance from the base to the first layer was 100 mm. After completing the construction of the model, horizontal displacements were measured using LVDT sensors installed at the top, bottom, and mid-height of the specimen.

3 NUMERICAL MODELING

To achieve a more realistic simulation and obtain a more reliable prediction of the model, the ABAQUS software, which is a finite element modeling (FEM) tool, was used. ABAQUS is widely employed in geotechnical engineering to simulate the mechanical behavior of soils and rocks. Its main advantages include the ability to model discrete and jointed media and to calibrate numerical parameters based on macroscopic laboratory test results. This numerical model was implemented to complement the experimental program, aiming to demonstrate the suitability of the observations derived from the laboratory for use in predictive numerical analyses. The model reproduces the experimental geometry, boundary conditions, and material properties, allowing an assessment of whether the deformation patterns and comparative behaviour observed experimentally can be consistently captured within a computational framework. It should be emphasized that the numerical simulations are not intended for parametric extrapolation or field-scale generalization; rather, they serve to illustrate the potential of integrating the laboratory results into subsequent modelling efforts, which reinforces the relevance and applicability of the experimental findings for predictive geotechnical analyses.

The numerical model was developed to simulate the behavior of a soil-reinforced wall with four reinforcement layers at a relative density of 50% for both reinforcement patterns. Figure 5 shows the distribution of horizontal displacements obtained from the ABAQUS simulations. The numerical results were compared with laboratory data recorded by the sensors. In defining the lateral boundaries of the numerical model, factors such as the type of analysis (static), soil properties, and specific boundary conditions of the software were considered. The analysis was performed under normal gravitational acceleration (1g), and a gravitational acceleration of 9.81 m/s² was defined in the model to replicate the laboratory conditions and ensure consistency between experimental and numerical simulations. Although it is generally recommended to set the lateral boundaries at three to five times the structure size to avoid stress reflections, in this study, the numerical domain dimensions were chosen to exactly match the laboratory model to enable direct comparison between numerical and experimental results. The properties of the soil materials defined in the numerical model are presented in Table 3.

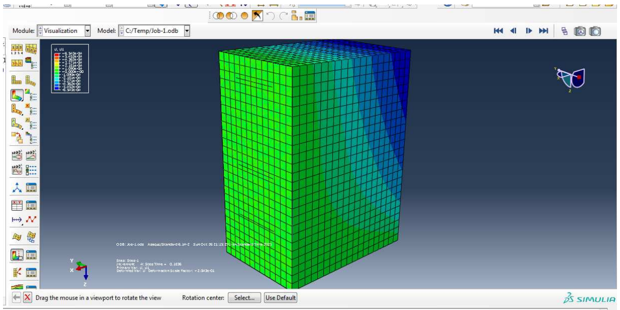

Figure 5. Horizontal displacement contours from the ABAQUS numerical simulation.

Table 3. Properties of the soil materials defined in the numerical modeling.

Soil	Young's modulus (kN/m^2)	Poisson's ratio (ν)	Unit weight (kN/m^3)	Friction angle (degree)	Cohesion (kPa)	Dilation angle (ψ)
Sand	3.5×10^3	0.25	16.2	39	5.5	4

4 RESULTS AND DISCUSSION

The horizontal displacements recorded by three LVDTs at the top, middle, and bottom levels of the laboratory model were compared with corresponding values from the numerical models, and the results are presented in Figures 6 and 7. At the LVDT1 level, the maximum horizontal displacement for the P/2 pattern in the laboratory model was 0.128 mm, while the corresponding value in the numerical model was 0.13 mm, showing a minor difference of 1.5% between the two. For the P/3 pattern, the laboratory and numerical displacements were 0.099 mm and 0.109 mm, respectively, indicating a 10% increase in displacement in the numerical model compared to the experimental one. At the LVDT2 level, the maximum horizontal displacement for the P/2 pattern was 0.067 mm in the laboratory model and 0.059 mm in the numerical model, reflecting about a 12% decrease in the numerical model. For the P/3 pattern, the corresponding values were 0.064 mm and 0.058 mm, showing approximately a 9% reduction in the numerical model. At the LVDT3 level, the maximum horizontal displacement for the P/2 pattern was 0.008 mm in the laboratory model and 0.017 mm in the numerical model, representing over 100% difference. For the P/3 pattern, the displacements were 0.014 mm and 0.02 mm, showing about a 43% difference. Based on these observations, the numerical model shows good agreement with the laboratory results at the middle and top levels, whereas larger discrepancies are observed at the bottom level. Furthermore, comparison of the two reinforcement patterns in both numerical and experimental models indicate smaller displacements for the P/3 pattern, demonstrating improved wall performance. This improvement is attributed to greater interlocking between the soil and the reinforcing sheets.

The maximum horizontal displacement at the top of the embankment in the laboratory model for the P/2 pattern was 0.128 mm, while for the P/3 pattern under the same surcharge, it was 0.076 mm. In other words, the maximum horizontal displacement for the P/3 pattern was approximately 73% lower than that of the P/2 pattern under identical loading conditions. Overall, the geometry and dimensions of the perforations in the reinforcement material are key factors influencing the deformation behavior of reinforced soil walls. Along with soil type, orientation, length, and number of reinforcement layers, and applied loading, the perforation pattern plays a significant role in the overall wall performance. One of the primary functions of the holes in the reinforcement layers is to influence stress distribution and the interaction between soil particles and the reinforcement. According to Albino et al. (2021), the presence of perforations promotes a more uniform distribution of tensile stresses along the reinforcement layer, thereby increasing load-bearing capacity and reducing stress concentration around the holes.

This study employed a small-scale 1g physical model where full stress similitude with prototype walls cannot be achieved. Vertical effective stresses develop solely from self-weight ($\sigma_v = \gamma H$), resulting in lower stress levels than full-scale walls due to reduced model height. Since soil stiffness and strength are stress-dependent, these confining stresses influence absolute deformation magnitudes and the relative stiffness between reinforcement (E_r) and soil (E_s). To systematically address scaling and similitude, Buckingham's π theorem was applied, expressing horizontal displacement u as a function of 12 parameters (Buckingham, 1914): wall height H, reinforcement length L_r, layer spacing S_v, perforation dimensions a and b, unit weight γ, friction angle φ, cohesion c, surcharge q, and elastic moduli E_s & E_r. This yields 9 dimensionless π-groups:

$$\frac{u}{H} = f\left(\frac{L_r}{H}, \frac{S_v}{H}, \frac{a}{H}, \frac{b}{H}, \frac{a}{b}, \frac{q}{\gamma H}, \frac{c}{\gamma H}, \frac{E_r}{E_s}, \varphi\right) \quad (1)$$

In the experimental setup, geometric ratios L_r/H and S_v/H are fixed, φ = 39°, c/(γH) ≈ 0.006 (low cohesion sand), and E_r/E_s ≈ 56. The primary variables are perforation aspect ratio a/b (2 for P/2, 3 for P/3) and normalized surcharge q/(γH). This dimensionless framework validates the comparative approach: at identical q/(γH), P/3 configuration reduces maximum u/H by 73% compared to P/2, confirming the perforation geometry's dominant role in deformation control. Rigid container boundaries may slightly alter lateral stresses compared to field conditions, but identical testing conditions across configurations ensure valid relative comparisons.

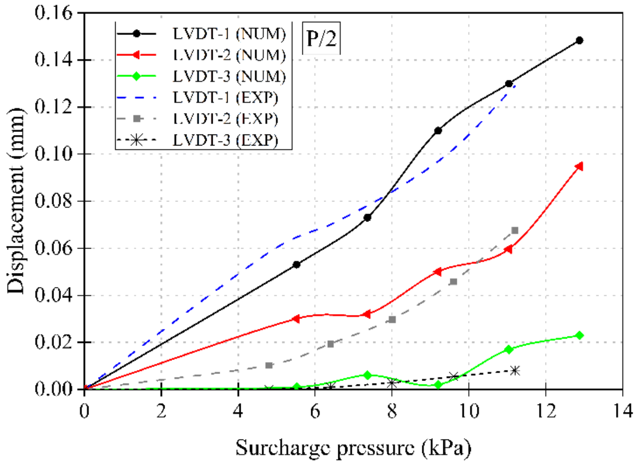

Figure 6. Comparison between numerical and experimental results of the reinforced soil wall with P/2 reinforcement pattern.

5 CONCLUSIONS

This study investigated the effect of the perforation pattern of reinforcement sheets on the deformation of a poorly graded sandy embankment using both numerical and experimental modeling. The results showed that, among the two patterns considered, the P/3 pattern produced smaller horizontal displacements in both the numerical and experimental models. Furthermore, the numerical and experimental models showed good agreement at the middle and upper levels of the embankment, whereas larger discrepancies were observed at the base, which can be attributed to differences between the actual boundary conditions in the laboratory model and those assumed in the numerical model.

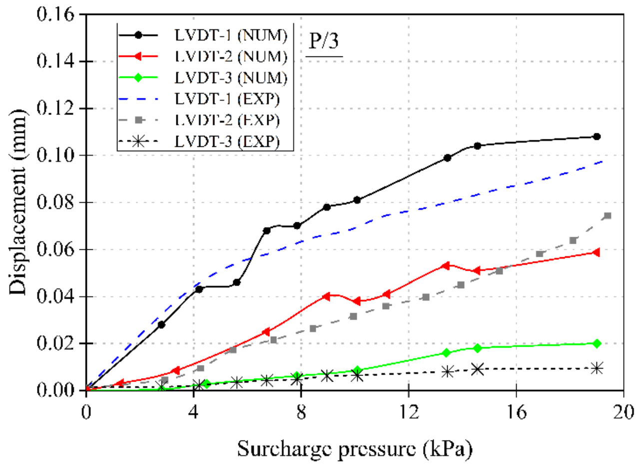

Figure 7. Comparison between numerical and experimental results of the reinforced soil wall with P/3 reinforcement pattern.

6 REFERENCES

Albino, J. L., R. C. Pierozan, and F. H. M. Portelinha. "Lateritic soil improved with partially reinforced granular columns using recycled sand and geosynthetics." International Journal of Geosynthetics and Ground Engineering 8, no. 2 (2022): 22. https://doi.org/10.1007/s40891-022-00367-1

ASTM Committee D6913 on Soil and Rock. Standard test methods for particle-size distribution (gradation) of soils using sieve analysis. ASTM International, 2009.

ASTM Committee D4253 on Soil and Rock. Standard Test Methods for Maximum Index Density and Unit Weight of Soils Using a Vibratory Table. ASTM International, 2021.

ASTM Committee D4254 on Soil and Rock. Standard Test Methods for Minimum Index Density and Unit Weight of Soils and Calculation of Relative Density. ASTM International, 2015.

Bathurst, Richard J., and Michael R. Simac. "Geosynthetic reinforced segmental retaining wall structures in North America." In Proceedings of the Fifth International Conference on Geotextiles, Geomembranes and Related Products, pp. 1-41. SEAC-IGA Singapore, 1994.

Bathurst, R. J., & Jamshidi Chenari, R. (2024). Design of geosynthetic MSE walls supporting bridge abutment footings using the stiffness method. In Geo-Congress 2024 (pp. 296-304). https://doi.org/10.1061/9780784485323.0

Bathurst, Richard J., and Michael R. Simac. "Geosynthetic reinforced segmental retaining wall structures in North America." In Proceedings of the Fifth International Conference on Geotextiles, Geomembranes and Related Products, pp. 1-41. SEAC-IGA Singapore, 1994.

Buckingham, E. (1914). On physically similar systems; illustrations of the use of dimensional equations. Physical review, 4(4), 345.

Cai, B., Cai, X., Li, S., Huang, X., Zhang, Y., & Xiao, C. (2025). Experimental study of shaking table for reinforced soil retaining walls: Analysis of tiered configuration effects. Soil Dynamics and Earthquake Engineering, 188, 109076. https://doi.org/10.1016/j.soildyn.2024.109076

Dash, Sujit Kumar. "Influence of relative density of soil on performance of geocell-reinforced sand foundations." Journal of Materials in Civil Engineering 22, no. 5 (2010): 533-538. https://doi.org/10.1061/(ASCE)MT.1943-5533.0000040

Dewoolkar, M. M., H-Y. Ko, and R. Y. S. Pak. "Experimental developments for studying static and seismic behavior of retaining walls with liquefiable backfills." Soil Dynamics and Earthquake Engineering 19, no. 8 (2000): 583-593. https://doi.org/10.1016/S0267-7261(00)00069-5

Ehrlich, M., S. H. Mirmoradi, and R. P. Saramago. "Evaluation of the effect of compaction on the behavior of geosynthetic-reinforced soil walls." Geotextiles and Geomembranes 34 (2012): 108-115. https://doi.org/10.1016/j.geotexmem.2012.05.005

Guler, E., Hamderi, M., & Demirkan, M. M. (2007). Numerical analysis of reinforced soil-retaining wall structures with cohesive and granular backfills. Geosynthetics International, 14(6), 330-345.https://doi.org/10.1680/gein.2007.14.6.330

Infante, Danny Useche, Gonzalo Aiassa Martinez, Pedro Arrúa, and Marcelo Eberhardt. "Behavior of geogrid reinforced sand under vertical load." GEOMATE Journal 10, no. 21 (2016): 1862-1868. https://doi.org/10.21660/2016.21.5168

Kayadelen, Cafer, Taha Ökkeş Önal, and Gökhan Altay. "Experimental study on pull-out response of geogrid embedded in sand." Measurement 117 (2018): 390-396. https://doi.org/10.1016/j.measurement.2017.12.024

Kim, Y. J., Jung, H. S., Lee, Y. J., Oh, D. W., Son, M., & Yoon, H. H. (2020). Behaviour analysis of reinforced soil retaining wall according to laboratory scale test. Applied Sciences, 10(3), 901. https://doi.org/10.3390/app10030901

Krishna, A. Murali, and G. Madhavi Latha. "Modeling the dynamic response of wrap-faced reinforced soil retaining walls." International Journal of Geomechanics 12, no. 4 (2012): 439-450. https://doi.org/10.1061/(ASCE)GM.1943-5622.0000128

Lee, K. Z. Z., N. Y. Chang, and H. Y. Ko. "Numerical simulation of geosynthetic-reinforced soil walls under seismic shaking." Geotextiles and Geomembranes 28, no. 4 (2010): 317-334. https://doi.org/10.1016/j.geotexmem.2009.09.008

Liu, Huifen, Huihuan Ma, Dan Chang, and Peiyuan Lin. "Statistical calibration of federal highway administration simplified models for facing tensile forces of soil nail walls." Acta Geotechnica 16, no. 5 (2021): 1509-1526. https://doi.org/10.1007/s11440-020-01106-4

Momeni, Ehsan, Akbar Yarivand, Mohammad Bagher Dowlatshahi, and Danial Jahed Armaghani. "An efficient optimal neural network based on gravitational search algorithm in predicting the deformation of geogrid-reinforced soil structures." Transportation geotechnics 26 (2021): 100446. https://doi.org/10.1016/j.trgeo.2020.100446

Pishgah, P., & Jamshidi Chenari, R. Some Rehabilitation Schemes for Geosynthetic-Reinforced Soil Abutments on Soft Soil Foundations. In Geo-Congress 2024 (pp. 350-358). https://doi.org/10.1061/9780784485323.0

Portelinha, F. H. M., J. G. Zornberg, and V. Pimentel. "Field performance of retaining walls reinforced with woven and nonwoven geotextiles." Geosynthetics International 21, no. 4 (2014): 270-284. https://doi.org/10.1680/gein.14.00014

Sharma, Vaibhav, and Arvind Kumar. "Influence of relative density of soil on performance of fiber-reinforced soil foundations." Geotextiles and Geomembranes 45, no. 5 (2017): 499-507. https://doi.org/10.1016/j.geotexmem.2017.06.004

Soleimanbeigi, A., A. Ozocak, B. Li, E. Akmaz, A. Y. Dayioglu, B. F. Tanyu, A. H. Aydilek, and W. J. Likos. "Mechanical and hydraulic compatibility of RAP with geosynthetics used in MSE walls." Geosynthetics International 29, no. 1 (2022): 1-18. https://doi.org/10.1680/jgein.21.00016

Touahmia, Mabrouk, Ahmed Rouili, Mustapha Boukendakdji, and Belkacem Achour. "Experimental and numerical analysis of geogrid-reinforced soil systems." Arabian Journal for Science and Engineering 43, no. 10 (2018): 5295-5303. https://doi.org/10.1007/s13369-018-3158-6

Vieira, Castorina S., and Paulo M. Pereira. "Influence of the geosynthetic type and compaction conditions on the pullout behaviour of geosynthetics embedded in recycled construction and demolition materials." Sustainability 14, no. 3 (2022): 1207. https://doi.org/10.3390/su14031207

Yang, Kuo-Hsin, Hsin-Ming Wu, Ting-Ling Tseng, and Chungsik Yoo. "Model tests of geosynthetic-reinforced soil walls with marginal backfill subjected to rainfall." Geotextiles and Geomembranes 51, no. 2 (2023): 342-359. https://doi.org/10.1016/j.geotexmem.2022.12.002

Yazdandoust, Majid. "Investigation on the seismic performance of steel-strip reinforced-soil retaining walls using shaking table test." Soil Dynamics and Earthquake Engineering 97 (2017): 216-232. https://doi.org/10.1016/j.soildyn.2017.03.011

Zheng, Yewei, John S. McCartney, P. Benson Shing, and Patrick J. Fox. "Physical model tests of half-scale geosynthetic reinforced soil bridge abutments. II: Dynamic loading." Journal of Geotechnical and Geoenvironmental Engineering 145, no. 11 (2019): 04019095. https://doi.org/10.1061/(ASCE)GT.1943-5606.0002158